

ORGANIC CHEMISTRY

Renewable lubricants with tailored molecular architecture

Sibao Liu¹, Tyler R. Josephson^{1,2}, Abhay Athaley^{1,3}, Qile P. Chen^{2,4}, Angela Norton^{1,5}, Marianthi Ierapetritou^{1,3}, J. Ilja Siepmann^{1,2,4}, Basudeb Saha^{1*}, Dionisios G. Vlachos^{1,5*}

We present a strategy to synthesize three types of renewable lubricant base oils with up to 90% yield using 2-alkylfurans, derived from nonfood biomass, and aldehydes, produced from natural oils or biomass through three chemistries: hydroxyalkylation/alkylation (HAA), HAA followed by hydrogenation, and HAA followed by hydrodeoxygenation. These molecules consist of (i) furan rings, (ii) saturated furan rings, and (iii) deoxygenated branched alkanes. The structures of these molecules can be tailored in terms of carbon number, branching length, distance between branches, and functional groups. The site-specific, energy-efficient C–C coupling chemistry in oxygenated biomass compounds, unmatched in current refineries, provides tailored structure and tunable properties. Molecular simulation demonstrates the ability to predict properties in agreement with experiments, proving the potential for molecular design.

INTRODUCTION

Lubricants are widely used in industrial machinery, automobiles, aviation machinery, refrigeration compressors, agricultural equipment, marine vessels, and many other applications and represent an over \$60 billion global chemical enterprise (1, 2). Base oils are key components [75 to 90 weight % (wt %)] of commercially formulated lubricants and account for up to 75% of lubricant cost (3). The majority of the current base oils are mineral oils (petroleum based), comprising a mixture of C₂₀–C₅₀ hydrocarbons and formulated with different additives [antioxidant, viscosity index (VI) improver, pour point (PP) depressant, corrosion inhibitors, antiwear reagents, and others] to achieve certain property specifications (1). These lubricants thicken quickly because they contain high-volatility, low-molecular weight hydrocarbons. As a result, frequent replacement is needed, which generates waste.

Better specifications can be achieved with synthetic base oils, such as poly- α -olefins (PAOs; Fig. 1A), alkylbenzenes, polyalkylenes, and synthetic esters (1). However, selectively tuning their molecular size and architecture is challenging (3). For example, cationic oligomerization of linear α -olefins (C₈–C₁₂ olefins), using homogeneous acid catalysts (BF₃, HF, or AlCl₃), results in uncontrolled oligomerization and formation of several products, which necessitate expensive separations following hydrogenation (3). In addition, homogeneous acid catalysts are corrosive. Reducing reliance on petroleum and mitigating the environmental footprint demand the production of high-performance lubricants from sustainable feedstocks (4–6). Biolubricants are produced using various chemical modifications of natural oils, i.e., animal fats and vegetable oils (7–10). High catalyst consumption, poor economics, and lack of effective heterogeneous catalysts (e.g., for hydroformylation) are common drawbacks in these transformations. Their structures result in high-temperature fluidity, low oxidative stability, and hydrolysis that limit their applicability. Similarly, recent strategies for the production of biolubricants, such as aldol condensation of alkyl methyl ketones or furanic molecules combined with hydrogenation or hydrodeoxygenation (HDO)

(11–13) and ether- and ester-based lubricants, using biomass-derived alcohol or levulinic acid (14–16), are challenged by the use of high amounts of catalyst, harsh reaction conditions, lack of control of architecture, and the need for separation of the homogeneous catalysts from the product for some reactions. Innovative approaches to synthesize biolubricant base oils with better and tunable properties can be transformative.

Here, we report a strategy to produce three broad classes of biolubricant base oils containing (i) furan rings with aromatic properties, (ii) fully saturated furan rings, and (iii) branched alkanes. These three products, hereafter referred to as furan-containing lubricant (FL), saturated FL (SFL), and bio-poly- α -olefin lubricant (BPAOL) base oils (Fig. 1B), are obtained via the hydroxyalkylation/alkylation (HAA) of 2-alkylfurans with aldehydes, HAA followed by hydrogenation, and HAA followed by HDO reactions, respectively. The C–C coupling of furans is a recently exploited reaction strategy to increase the carbon chain and produce diesel and jet fuels (17–21), but its adaptation to produce biolubricant base oils is still in its infancy. The synthesis of 2-alkylfurans of different carbon numbers via direct HDO of C₅ sugars of biomass (22), i.e., 2-methylfuran (2MF), or furan acylation with carboxylic acids (or their anhydrides) followed by HDO of the acylated products (scheme S1) (23) has been reported. Similarly, aldehydes of different carbon lengths can be synthesized via dehydrogenation of biomass-derived alcohols (24) or selective hydrogenation of fatty acids from natural oils or waste cooking oils (WCO) (25). The use of alkylfurans and aldehydes of varying carbon lengths and branching enables the synthesis of lubricant base oils of different molecular sizes, structures, branching sizes, and distances between branches. This enables unprecedented flexibility in tuning lubricant specifications for a wide range of applications that are currently achieved by complex formulation of mineral and synthetic base oils with chemical additives. Their well-defined structure also enables the application of molecular simulation to predict the base oil properties, such as viscosity and VI, and to direct the design and synthesis of new lubricant base oils with desirable properties.

RESULTS

First, we synthesized C₃₀-FL1, a furan-containing base oil whose rings have aromatic properties. Furan-based oils have no analogs in the crude oil-based economy. C₃₀-FL1 contains the same number of carbon

¹Catalysis Center for Energy Innovation, Newark, DE 19716, USA. ²Department of Chemical Engineering and Materials Science, University of Minnesota, Minneapolis, MN 55455, USA. ³Department of Chemical and Biochemical Engineering, Rutgers, The State University of New Jersey, NJ 08854, USA. ⁴Department of Chemistry, University of Minnesota, Minneapolis, MN 55455, USA. ⁵Department of Chemical and Biomolecular Engineering, University of Delaware, Newark, DE 19716, USA.

*Corresponding author. Email: bsaha@udel.edu (B.S.); vlachos@udel.edu (D.G.V.)

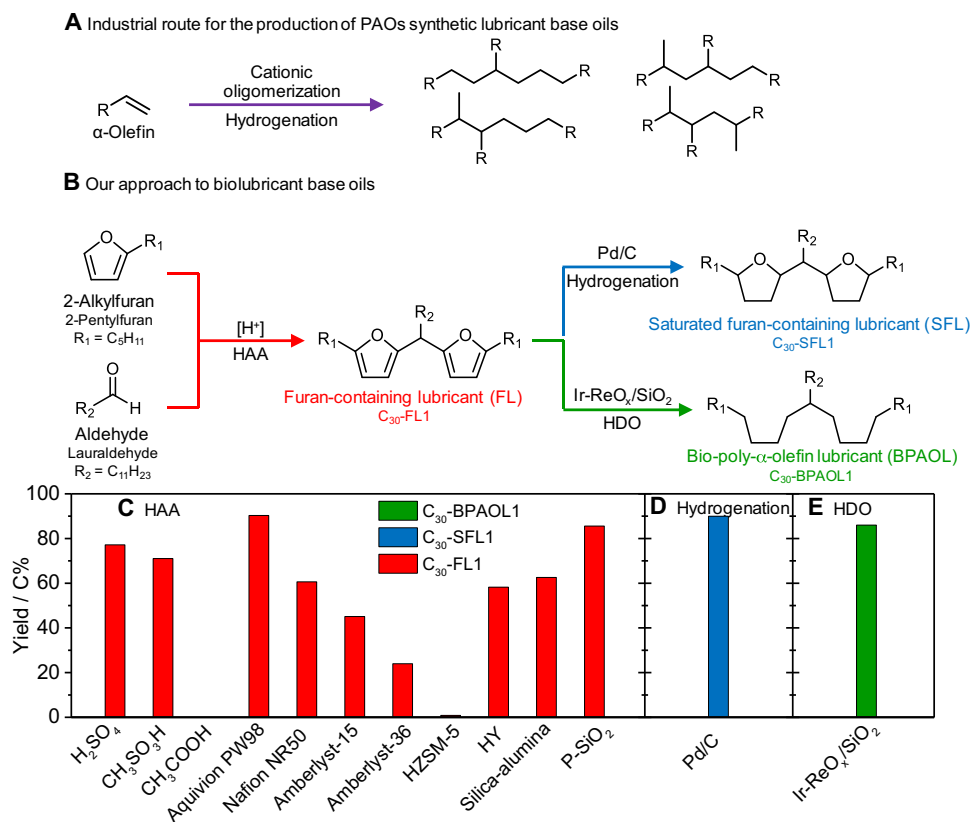


Fig. 1. Commercial and proposed routes for the production of lubricant base oils. (A) Industrial route for the production of PAOs synthetic lubricant base oils. (B) Proposed approach to biolubricant base oils. HAA of biomass-derived 2-alkylfuran with an aldehyde produces FL base oils. Hydrogenation of FL over Pd/C gives SFL base oils. HDO of FL over Ir-ReO_x/SiO₂ produces BPAOL base oils. (C) C₃₀-FL1 yields from HAA reaction of 2-pentylfuran with lauraldehyde over various acid catalysts: 10 mmol 2-pentylfuran, 5 mmol lauraldehyde, and 0.05 mmol H⁺, e.g., 0.05 g of Aquivion PW98, 65°C, 6 hours. (D) Hydrogenation results of C₃₀-FL1 to C₃₀-SFL1 over Pd/C catalysts: 0.5 g of C₃₀-FL1, 0.03 g of Pd/C, 6 MPa H₂, 60°C, 2 hours. (E) HDO of C₃₀-FL1 to C₃₀-BPAOL1 over an Ir-ReO_x/SiO₂ catalyst: 0.3 g of C₃₀-FL1, 0.15 g of catalyst, 5 MPa H₂, 170°C, 12 hours.

atoms as a C₃₀ alkane, a major compound in commercial PAO synthetic base oils. Selective hydrogenation of FL1 leads to SFL1. Neither FL1 nor SFL1 is in the current portfolio of mineral oils or synthetic base oils. Last, HDO of FL1 produces C₃₀-BPAOL1 that is compositionally identical to C₃₀ alkane in commercial PAOs. For the HAA reaction, the screening of homogeneous catalysts (sulfuric acid, methanesulfonic acid, and acetic acid) was conducted using 2-pentylfuran and lauraldehyde as substrates (Fig. 1B). The former substrate can be produced from acylation of furan with valeric acid or valeric anhydride followed by HDO (23). The latter can be synthesized from lauric acid of coconut oil by selective hydrogenation (25). Sulfuric and methanesulfonic acid achieve up to 77% yield of C₃₀-FL1 under neat conditions at a 2:1 molar ratio of 2-pentylfuran and lauraldehyde (Fig. 1C and fig. S1; the experimental procedure and product analysis are in the Supplementary Materials). In contrast, acetic acid is ineffective (18, 19). Despite the activity of these catalysts, their separation and disposal are challenging and can render biolubricant base oils corrosive.

To overcome the aforementioned challenges, we evaluated the potential of solid sulfonic acid resins, e.g., perfluorinated sulfonic acid resins (Aquivion PW98, Nafion NR50) and sulfonic acid-functionalized cross-lined polystyrene resins (Amberlyst-15 and Amberlyst-36). The catalytic performance follows the order of Aquivion PW98 > Nafion NR50 > Amberlyst-15 > Amberlyst-36.

A 90% yield with >98% selectivity to C₃₀-FL1 is achieved in 6 hours, at 65°C and neat condition, using 0.05 g of Aquivion PW98 due to its strong acid strength and high surface area (table S1) (18, 19). Reaction conditions, such as reaction time, catalyst amount, and reaction temperature, have been optimized (figs. S2 to S4). The dominant product is C₃₀-FL1 along with a small amount of C₂₁H₃₈O₂, an intermediate formed in the first step (hydroxyalkylation), suggesting that the reaction follows a tandem pathway (scheme S2) and alkylation is faster than hydroxyalkylation, as reported in the literature (21). A slightly higher yield (92%) is achieved after 8 hours (fig. S2). The apparent activation energy (*E*_A) of the overall reaction is 16 kJ mol⁻¹ (fig. S4). Controlled experiments show no leaching of acid sites in the solution and almost constant catalytic performance of Aquivion PW98 up to four consecutive cycles (fig. S6). About 30% activity loss occurs in the fifth cycle with concurrent mass gain and brown coloration of the recovered Aquivion PW98, indicating blocking of the acid sites of the catalyst by the viscous condensation product. Aquivion PW98 is not thermally stable at >160°C, which makes regeneration by traditional calcination impossible.

Next, microporous acid zeolites (HZSM-5 and HY) were evaluated. HY gives a moderate yield (58%) of C₃₀-FL1, whereas HZSM-5 is ineffective (<1% C₃₀-FL1) (Fig. 1C). Since diffusion limitations are expected for large molecules in microporous zeolites, we chose a mesoporous aluminosilicate with a pore diameter of ~5.4 nm. The

aluminosilicate catalyst exhibits comparable performance as HY, likely due to the larger pore diameter being counterbalanced by a lower acid strength in a noncrystalline environment (13). In recent work, P-containing zeolites with unique acid properties were reported (26–28). A P-containing mesoporous siliceous (P-SiO₂) catalyst, prepared by simple impregnation, exhibits superior performance to mesoporous aluminosilicate and yields C₃₀-FL1 comparable to Aquivion PW98 in a much shorter reaction time (1.5 hours versus 6 hours) (figs. S1 and S7). Homogeneous phosphoric acid shows no activity, even with double the amount of P concentration. No reaction occurs using the filtrate of the catalyst, indicating that P-SiO₂ functions as a heterogeneous catalyst (fig. S7). Product condensation (fig. S9) with concurrent dark brown coloration caused a loss of catalytic activity in the second cycle (fig. S8). The regenerated P-SiO₂, upon calcination at 500°C in air for 3 hours, regains comparable performance to the fresh catalyst (fig. S8).

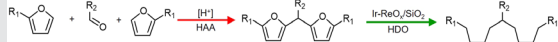
Next, we refine the C₃₀-FL1 either by hydrogenation or by HDO to produce C₃₀-SFL1 and C₃₀-BPAOL1 base oils, respectively (Fig. 1, D and E). A commercial Pd/C catalyst was used for the former under mild reaction conditions, as Pd is active for furan ring hydrogenation (29). Reaction time and hydrogen pressure experiments (fig. S10) suggest that a high hydrogen pressure facilitates ring saturation with an optimum yield of C₃₀-SFL1 of ~90%.

C₃₀-FL1 HDO over an Ir-ReO_x/SiO₂ catalyst, which demonstrated excellent catalytic performance for furan ring opening and deoxygenation (30) via synergy of Ir hydrogenation sites and acidic sites of partially reduced ReO_x, yields 86% C₃₀-BPAOL1 (Fig. 1E). Small fractions of C₂₁- and C₉-alkanes form via C–C cracking. The regeneration of the catalyst by calcination before each cycle demonstrates comparable performance in five consecutive runs (figs. S12 and S13). Notably, C₃₀-FL1, SFL1, and BPAOL1 base oils form with high selectivity, minimizing expensive and complex separations associated with commercial mineral and synthetic base oils.

The proposed synthetic platform is general. We demonstrate this using 2-alkylfurans and aldehydes of different carbon lengths and substituents, using Aquivion PW98 and P-SiO₂ as the HAA catalysts, followed by HDO of the products over the Ir-ReO_x/SiO₂ catalyst (Table 1 and table S2). Both the Aquivion PW98 and P-SiO₂ catalysts exhibit similar performance with yields of FLs of 80 to 94% depending on the molecular sizes. Similarly, HDO of FLs yields 81 to 91% BPAOLs depending on the molecular sizes of FLs and the lengths of alkyl groups of 2-alkylfurans and aldehydes. The formation rates of C₂₆–C₃₀ FLs at low conversion (<25%) linearly decrease with increasing alkyl chain length of 2-alkylfurans or aldehydes, but the effect of size on rate is not dramatic (figs. S14 and S15). Our C₂₀- and C₃₀-BPAOLs have structural similarity with current commercial PAO2 and PAO4 lubricant base oils to enable direct comparison of properties.

Base oils with multiple branches have lower PPs for low-temperature applications, e.g., refrigeration and aircrafts. HAA reaction of 2-alkylfuran with branched aldehydes, e.g., 2-ethylhexanal, which can be obtained by dehydrogenation of Guerbet alcohols, forms C₂₆–C₃₀ FLs (Table 1, entries 12 to 14). High yields of C₂₆–C₃₀ FLs were achieved over both Aquivion PW98 and P-SiO₂ catalysts (Table 1, entries 12 to 14, and table S2, entries 12 to 14). The formation rate of C₂₆-FL3 with two branches is three times lower than that of C₂₆-FL2 with one branch (fig. S16), likely due to a steric hindrance during the condensation arising from the additional branching of 2-ethylhexanal. HDO over Ir-ReO_x/SiO₂ produces C₂₆–C₃₀ BPAOLs in high yield (Table 1, entries 12 to 14).

Table 1. Synthesis of FL and BPAOL base oils using 2-alkylfurans and aldehydes of varying molecular sizes. Reaction conditions: HAA reactions of 2-alkylfurans with aldehyde to FL were conducted using 0.05 g of Aquivion PW98, 10 mmol 2-alkylfuran, and 5 mmol aldehyde at 65°C for 6 hours. HDO of FL to the corresponding BPAOL over the Ir-ReO_x/SiO₂ catalyst was performed using 0.3 g of FL in 10 ml of cyclohexane solvent and 0.15 g of catalyst at 5 MPa H₂ and 170°C for 12 hours.



Entry	Reagents		HAA reaction		HDO reaction	
	R ₁	R ₂	Products	Yield (%)	Products	Yield (%)
1	Methyl	<i>n</i> -Undecyl	C ₂₂ -FL1	80	C ₂₂ -BPAOL1	91
2	Ethyl	<i>n</i> -Undecyl	C ₂₄ -FL1	82	C ₂₄ -BPAOL1	85
3	<i>n</i> -Propyl	<i>n</i> -Undecyl	C ₂₆ -FL1	94	C ₂₆ -BPAOL1	87
4	<i>n</i> -Butyl	<i>n</i> -Undecyl	C ₂₈ -FL1	89	C ₂₈ -BPAOL1	84
5	<i>n</i> -Pentyl	<i>n</i> -Undecyl	C ₃₀ -FL1	90	C ₃₀ -BPAOL1	87
6	<i>n</i> -Hexyl	<i>n</i> -Undecyl	C ₃₂ -FL1	89	C ₃₂ -BPAOL1	82
7*	<i>n</i> -Heptyl	<i>n</i> -Undecyl	C ₃₄ -FL1	85	C ₃₄ -BPAOL1	83
8	<i>n</i> -Pentyl	Methyl	C ₂₀ -FL1	89	C ₂₀ -BPAOL1	87
9	<i>n</i> -Pentyl	<i>n</i> -Pentyl	C ₂₄ -FL2	93	C ₂₄ -BPAOL2	89
10	<i>n</i> -Pentyl	<i>n</i> -Heptyl	C ₂₆ -FL2	91	C ₂₆ -BPAOL2	91
11	<i>n</i> -Pentyl	<i>n</i> -Nonyl	C ₂₈ -FL2	87	C ₂₈ -BPAOL2	87
12 [†]	<i>n</i> -Pentyl	2-Ethylpentyl	C ₂₆ -FL3	85	C ₂₆ -BPAOL3	87
13 [†]	<i>n</i> -Hexyl	2-Ethylpentyl	C ₂₈ -FL3	86	C ₂₈ -BPAOL3	82
14 [†]	<i>n</i> -Heptyl	2-Ethylpentyl	C ₃₀ -FL2	88	C ₃₀ -BPAOL2	81

*Eight hours. †Twelve hours.

Important properties {VI, PP, volatility [thermogravimetric analysis (TGA) Noack] and oxidation stability} of C₃₀-FL1, C₃₀-SFL1, and C₃₀-BPAOL1 base oils are compared with those of commercial mineral group II and PAO4 group IV base oils, categorized by the American Petroleum Institute in Table 2. Our C₃₀ base oils have better volatility than commercial base oils, while the VIs of C₃₀-FL1 and C₃₀-SFL1 are comparable or slightly lower than those of the commercial products because of the presence of furan and tetrahydrofuran rings in the structures. C₃₀-SFL1 has higher KV_s and VI than C₃₀-FL1, indicating that molecular structure and oxygen content strongly affect these properties. The oxidation stability of C₃₀-SFL1 and C₃₀-FL1 is lower than that of commercial PAO4, but their PPs are comparable to those of commercial PAO4, making them suitable for low-temperature applications. The hydrophilic ring improves the polarity of base oils, which is beneficial for their solubility with polar additives, which is currently a challenge (1). The PP of C₃₀-BPAOL1 is better than that of mineral group II base oil, with C₃₀-BPAOL1 having superior VI than commercial group II and synthetic PAO4 base oils (high VI ensures low viscosity changes with temperature). The PP of BPAOL3 is expected to be even lower because of the two branches in its molecular structure. The biodegradability of our lubricants is yet to be determined, but our synthesized biolubricants could lead to low fossil carbon use and reduced CO₂ emissions.

Table 2. Properties of C₃₀-FL1, SFL1, and BPAOL1 base oils compared with those of select commercial formulated lubricants. N/A, not applicable.

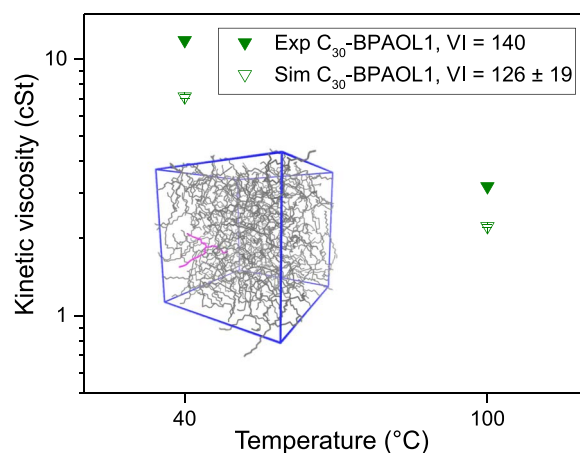
Lubricant base oils	KV ₁₀₀ * (cSt)	KV ₄₀ * (cSt)	VI†	PP‡ (°C)	Noack volatility§ (wt %)	DSC oxidation onset Temperature (°C)
C ₃₀ -FL1	3.14	12.91	105	<−63	10	170
C ₃₀ -SFL1	3.91	17.92	113	<−60	11.5	154
C ₃₀ -BPAOL1	3.19	11.84	140	−21	13.8	201
ExxonMobil PAO4	4.1	19.0	126	−66	18.8	221
Group II (150 N)¶	5.3	30.6	106	−13	14.5	N/A

*KV₁₀₀ and KV₄₀ are kinematic viscosities at 100° and 40°C, respectively (ASTM D445). †VI calculated from KV₁₀₀ and KV₄₀ (ASTM D2270). ‡PP (ASTM D97). §Volatility (ASTM D6375). ||Oxidation stability (ASTM E2009, method B, 500 pis O₂). ¶Mineral group II base oil.

The proposed synthetic platform provides unprecedented control over the molecular size of nearly monodispersed (C₂₂–C₃₄) lubricant base oils with site-specific branching (Table 1). This control arises from the selective acylation at the alpha carbon of the furan in producing alkyl-furans and the site-specific C–C coupling of the HAA chemistry on the opposite alpha carbon of the 2-alkylfuran. This site specificity is lacking from olefins, whose oligomerization and C=C bond migration lead to a broad distribution of products. As a result, the oxygen of biomass opens up opportunities for site-specific C–C coupling strategies, unmatched in hydrocarbon chemistry in refineries. As a result, product specifications can be unique and allow targeting various applications easily. Our strategy enables the synthesis of molecules with very narrow size distribution as compared with commercial products (fig. S17). This narrow molecular weight distribution provides another opportunity for molecular design of these products. Molecular simulation is an ideal tool to estimate properties of tailored molecules (31–35) using high-performance computing. In turn, this can enable inverse engineering so molecules with specific properties can be designed on the computer. We used equilibrium molecular dynamics (MD) to demonstrate the feasibility of this approach by predicting the viscosities and VI of five representative C₃₀-BPAOL lubricant base oils (table S3).

The experimental viscosity of C₃₀-BPAOL1 is used to benchmark the accuracy of the simulations. The predicted kinematic viscosities at 40° and 100°C are 7.1 ± 0.1 and 2.23 ± 0.03 cSt, respectively, underpredict the experimental viscosities of 11.84 and 3.19 by ~20% (Fig. 2). Previous studies have also found that united-atom force fields underpredict the experimental viscosities of alkanes (32–35). The calculated VI of 126 ± 19 is slightly lower than the experimental VI of 140.

To probe the effects of architecture and branching on viscosities and VI, we also simulated four additional C₃₀-BPAOL base oil molecules with a variety of branching (table S3). The predicted viscosities of four isomers with a single branch point vary by only 10% at 40°C but this spread increases to 20% at 100°C, leading to VIs that range from 116 ± 26 for BPAOL4 to 227 ± 14 for BPAOL3. The VI of BPAOL3 with a short pentyl side chain at position 6 is predicted to be significantly higher than the others, but may also be accompanied by an increased PP due to its relatively elongated structure (1). These differences arise from differences in torsional diffusivity and rotational relaxation times associated with differences in molecular architecture (32, 34). The additional branching of BPAOL2 reduces the predicted viscosity relative to BPAOL1 without significantly affecting the pre-

**Fig. 2. Comparison of experimental (Exp) and predicted (Sim) by molecule simulation kinematic viscosities at 40° and 100°C.**

dicted VI compared with the single-branched isomers with heptyl or longer side chains. The additional branching is also likely to reduce the PP, although there is no method yet for predicting PP using molecular simulation. Expanding these simulations to a library of potential molecules could direct synthesis efforts.

Technoeconomic analysis predicts the selling price of C₃₀-BPAOL1 to be \$5191/metric ton using commercial furfural as a feedstock and \$4535/metric ton using furfural obtained from a biorefinery in which cellulose from deconstructed lignocellulosic biomass is converted to *p*-xylene and lignin (constituting ~20 wt % of dry weight of biomass). Lignin is considered as a waste stream with no value (detailed analysis, process block flow diagram, and assumptions are given in the Supplementary Materials). The price of our product, which is expected to be even lower upon consideration of a reasonable price for lignin value, is very competitive with the price of current commercial synthetic PAO4 (~\$4475/metric ton) provided by a business insider from the J.A.M. Distributing Company. A higher price premium of our products is expected for synthesizing designer molecules, guided by MD simulation, with desired specifications for targeted applications that will likely minimize the use of expensive chemical additives required for formulation, and branding the products as environmentally acceptable lubricants (EALs) upon biodegradability testing. Some premium EALs, e.g., gear, stern tube, and hydraulic oils manufactured by GulfSea,

are currently sold at \$15 to \$17/liter, i.e., at a price significantly higher than that of our products.

DISCUSSION

We demonstrated a strategy to synthesize new and existing lubricant base oils with structural diversity and excellent control over molecular weight, size distribution, and branching using energy-efficient C–C coupling without complex separations needed for current petroleum-based base oils. Nonfood biomass and natural or WCO can be harnessed to obtain synthons (alkylfurans and aldehydes) of varying carbon lengths and branching for various targeted applications. Efficient and easily separable heterogeneous catalysts enable high product selectivity and yield (up to 95%). In addition, low-temperature processing compared with the current refinery processing (cracking, isomerization, and distillation for synthetic and mineral base oils) and use of sustainable, abundant feedstock provide a sustainable route to biolubricants. Structural control enables tuning of product properties, and use of one-step chemistry (HAA) or two-step chemistry (HAA followed by HDO) leads to diverse classes of products with aromatic rings (FL), oxygen-containing cyclic rings (SFL), or branched alkanes (BPAOL). C₃₀ products, chosen for demonstration, have comparable or better properties than the current commercial mineral or synthetic base oils. The properties can be predicted by molecular simulation to inform design of molecules, an approach previously unavailable for petroleum-derived base oils that cannot be synthesized with molecular specificity.

MATERIALS AND METHODS

Materials

Aquivion PW98 [coarse powder, Brunauer-Emmett-Teller (BET) surface area <1 m²/g, and 1.0 mmol H⁺/g] (36), Nafion NR50 (pellets, BET surface area <1 m²/g, and 0.89 mmol H⁺/g) (37), Amberlyst-15 (dry hydrogen form; pore size, 34.3 nm; BET surface area, 42 m²/g; and 4.8 mmol H⁺/g) (38), amorphous silica alumina (ASA; catalyst support grade 135; 12 wt % Al₂O₃; >90% AS-100 mesh; pore size, 5.4 nm; BET surface area, 569 m²/g; and 0.34 mmol H⁺/g) (39), methanesulfonic acid (≥99.0%), acetic acid, silica gel (high-purity grade; pore size, 6 nm; and 70 to 230 mesh), 2-pentylfuran (≥98.0%), 2MF (99%), 2-ethylfuran (≥99.0%), lauraldehyde (≥95%), hexanal (98%), octanal (99%), decanal (≥98.0%), 2-ethylhexanal (96%), eicosane (99%), Pd/C (10 wt % Pd loading), and H₂IrCl₆ (99.98%, trace metal basis) were purchased from Sigma-Aldrich. 2-Propylfuran (>98%) and 2-butylfuran (>98%) were purchased from Tokyo Chemical Industry Co. Ltd. 2-Hexylfuran (97%) and 2-heptylfuran (97%) were purchased from Alfa Aesar. Amberlyst-36 dry resin (pore size, 32.9 nm; BET surface area, 33 m²/g; and 5.4 mmol H⁺/g) (38) was purchased from the Rohm and Haas Company. H₂SO₄ (5 M) was purchased from Fluka. *o*-Phosphoric acid (85%) and cyclohexane (99.9%) were purchased from Fisher Chemical. Ammonium perrhenate(VII) (99.999%, metals basis) was purchased from Alfa Aesar. Silica gel G6 (BET surface area, 535 m²/g) was provided by Fuji Silysia Chemical Ltd. The commercial ZSM-5 (CBV2314; Si/Al = 11.5; pore size, ~0.5 nm; BET surface area, 425 m²/g; and 0.65 mmol H⁺/g) (40) and HY (CBV720; Si/Al = 15; pore size, ~0.7 nm; BET surface area, 780 m²/g; and 0.31 mmol H⁺/g) (39) were purchased from Zeolyst.

Material pretreatment

2-Alkylfurans (2MF, 2-ethylfuran, 2-propylfuran, 2-butylfuran, 2-pentylfuran, 2-hexylfuran, and 2-heptylfuran) were purified by

vacuum distillation. The zeolites ZSM-5 and HY were calcined at 550°C for 4 hours at a heating rate of 2°C/min. The ASA was calcined before use for 10 hours at 500°C at a heating rate of 2°C/min under static air. The silica gels were calcined in air at 700°C for 1 hour at a heating rate of 10°C/min before catalyst impregnation.

Catalyst preparation

The P-SiO₂ catalyst (H₃PO₄, 10 wt % loading) was prepared by impregnation. First, SiO₂ (Sigma-Aldrich) was impregnated by aqueous H₃PO₄ solution. After evaporating the solvent at 75°C on a hotplate and subsequently drying at 110°C for 12 hours in an oven, the catalyst was calcined in a crucible in air at 500°C for 3 hours with a 2°C/min temperature ramp. The Ir-ReO_x/SiO₂ (Ir, 4 wt % loading; Re/Ir = 2 M) catalyst was prepared using sequential impregnation. First, Ir/SiO₂ was prepared by impregnating Ir on SiO₂ (Fuji Silysia G-6) using an aqueous solution of H₂IrCl₆. After evaporating the solvent at 75°C on a hotplate and drying at 110°C for 12 hours in an oven, the resulting Ir/SiO₂ was impregnated with ReO_x using an aqueous solution of NH₄ReO₄. The catalysts were calcined in a crucible in air at 500°C for 3 hours with a 10°C/min temperature ramp. The reported metal loadings in the catalysts were based on the theoretical amount of metals used in impregnation.

Reaction procedures

HAA reaction

In a typical reaction, 10 mmol 2-alkylfuran and 5 mmol aldehyde without any solvent were mixed in a 20-ml glass vial. The vial was placed in a preheated oil bath and stirred at 500 rpm using a magnetic bar on a stirring cum hotplate. Last, the catalyst was added into the vial, and the reaction continued at the desired temperature (65°C unless otherwise mentioned) for 6 hours. After the reaction, the solution was diluted using 10 ml of cyclohexane solvent. A small amount of eicosane was added as an internal standard.

HAA rate measurements

Because different 2-alkylfurans and aldehydes have different densities and their mixing without a solvent changes the volume for different reactions, we used cyclohexane as the solvent for the measurement of reaction rates. Typically, 10 mmol 2-alkylfuran and 5 mmol aldehyde were dissolved in cyclohexane, and their concentrations were kept at 1 and 0.5 mol/liter, respectively. The reactions were performed in the same way as HAA reactions described above. After the reaction, the solution was diluted with 10 ml of cyclohexane containing a small amount of eicosane as an internal standard.

Hydrogenation reaction

Hydrogenation of HAA condensation products, hereto referred to as unsaturated FLs, was carried out in a 50-ml Parr reactor with an inserted Teflon liner and a magnetic stirrer. First, Pd/C catalyst was pretreated at 200°C with a temperature ramp of 10°C/min for 1 hour with H₂ (50 ml/min). Then, Pd/C catalyst (0.03 g), FL (0.5 g), and 10 ml of cyclohexane were added to the reactor, and the mixture was heated at 60°C. Upon completing the reaction, the reactor was immediately transferred to an ice-water bath. Upon cooling down the solution to room temperature, the reactor was opened, the solution was diluted using 10 ml of cyclohexane containing a small amount of eicosane as an internal standard, and the catalyst was separated from the solution by filtration.

HDO reaction

HDO of FLs over Ir-ReO_x/SiO₂ was performed in a 50-ml Parr reactor with an inserted Teflon liner and a magnetic stirrer. First, the catalyst (0.15 g) and solvent (10 ml of cyclohexane) were added to the reactor for catalyst prereduction, and the reactor was sealed with the reactor head

equipped with a thermocouple, a rupture disk, a pressure gauge, and a gas release valve. The mixture was heated at 200°C and 5 MPa H₂ for 1 hour at 240 rpm. Upon prereduction, the reactor was cooled to room temperature and H₂ was released. Then, we added FLs (0.3 g), closed the reactor head immediately, purged the reactor with 1 MPa H₂ for three times, pressurized to 5 MPa H₂, and heated the reaction mixture to the desired temperature with continuous stirring at 500 rpm. The heating time to reach the set temperature was about 25 min. Upon reaction, the reactor was immediately transferred to a water bath. The reaction solution was diluted using 15 ml of cyclohexane with a small amount of eicosane as an internal standard, and the catalyst was separated from the solution by centrifugation or filtration.

Analysis of products

The products were analyzed using a gas chromatograph (GC, Agilent 7890A) equipped with an HP-1 column and a flame ionization detector using eicosane (C₂₀) as an internal standard. The products were identified by a GC (Agilent 7890B) mass spectrometer (MS) (Agilent 5977A with a triple-axis detector) equipped with a DB-5 column, high-resolution MS with liquid injection field desorption ionization, ¹H nuclear magnetic resonance (NMR), and ¹³C NMR (Bruker AV400, CDCl₃ solvent).

The conversion and the yield of all products from the HAA, hydrogenation, and HDO reactions were calculated on a carbon basis using the following equations

$$\text{Conversion}[\%] =$$

$$\frac{\text{mol of initial reactant} - \text{mol of unreacted reactant}}{\text{mol of initial reactant}} \times 100$$

$$\text{Yield of detected products}[\%-\text{C}] =$$

$$\frac{\text{mol}_{\text{product}} \times \text{C atoms in product}}{\text{mol of total C atoms of initial reactants}} \times 100$$

Lubricant properties

The lubricant properties of select C₃₀ compounds (C30-FL1, C30-SFL1, and C30-BPAOL1) were evaluated according to American Society for Testing and Materials (ASTM) methods. The kinematic viscosities at 100° and 40°C (KV100 and KV40) were determined using the ASTM D445 method. The VI was calculated using the KV100 and KV40 following the ASTM D2270 method. The PP tests were carried out according to ASTM D97. The kinematic viscosities and PP measurements were performed at Southwest Research Institute in San Antonio, Texas, USA. The differential scanning calorimetry (DSC) oxidation onset temperature and Noack volatility were measured according to ASTM E2009 (method B, 500 pis O₂) and ASTM D6375, respectively, at Petro-lubricant Testing Laboratories Inc. in Lafayette, NJ, USA.

Characterizations

The TGA of the fresh and used P-SiO₂ catalysts was performed on a TA Q600 HT TGA/DSC. The microstructures of the fresh and used catalysts (Pd/C and Ir-ReO_x/SiO₂) were examined using the field emission transmission electron microscope JEM-2010F FasTEM at 200 kV.

MD simulations

MD simulations in the NVT ensemble were performed using the GROMACS 5.0.0 software (41, 42). The lubricants were modeled

using the TraPPE-UA force fields (43, 44), with a carbon-carbon bond force constant of 376,500 kJ mol⁻¹ nm⁻². A 14-Å cutoff was used with the analytical tail correction (45). The number of molecules was $N = 170$ for all lubricants studied. The volume V and initial structures were generated using Monte Carlo (MC) simulations in the NpT ensemble for 2×10^5 MC cycles (one MC cycle consisting of N randomly selected MC steps). MC simulations were run using the MC for Complex Chemical Systems–Minnesota software program (46) with the k -d tree data structure (47). Center-of-mass translation, center-of-mass rotation, conformational (44), and volume moves were used to equilibrate the system at desired T and $p = 1$ atm. Four independent MD simulations were performed starting from different initial structures. A time step of 2 fs was used, and the pressure tensor was output every two time steps. A Nosé-Hoover thermostat (48, 49), with a coupling time constant of 5 ps, was used to control temperature. Each simulation lasted for at least 1500 ns. The initial part (first 100 ns) of each trajectory was discarded, and the remainder was used for analysis. The method developed by Zhang *et al.* (50) was used to obtain the viscosity for each independent run using the Green-Kubo integral (51) with a block size of 10 ns. Uncertainties were calculated as SEM from eight independent simulations and were reported as 95% confidence intervals. Viscosities obtained at 313 and 373 K were used to calculate the VI using ASTM D2270. Simulation snapshots were visualized using visual molecular dynamics (52) and Tachyon (53).

Technoeconomic analysis

Using the available data, a simulation of the production processes was performed using Aspen Plus version 8.8.2. The nonrandom two-liquid method was used to predict the liquid-liquid and liquid-vapor behaviors. Most of the components involved in the reactions were directly selected from the Aspen database. The components not found in the database (i.e., synthesized furan compounds and lubricants) were defined by their structures. All missing parameters were estimated by the molecular structures using the UNIFAC Model and Thermo Data Engine (TDE). TDE is a thermodynamic data correlation, evaluation, and prediction tool developed by the collaboration of Aspen Plus and the National Institute of Standard and Technology (54). The detailed analysis, process block flow diagram, and assumptions (55–62) are given in the Supplementary Materials.

SUPPLEMENTARY MATERIALS

Supplementary material for this article is available at <http://advances.sciencemag.org/cgi/content/full/5/2/eaav5487/DC1>

Scheme S1. Strategies for the synthesis of 2-alkylfurans.

Scheme S2. Reaction pathway for HAA of 2-alkylfuran with an aldehyde over acid catalyst.

Table S1. Properties of commercial solid acid catalysts.

Table S2. HAA reaction of different 2-alkylfurans with aldehydes over P-SiO₂.

Table S3. Simulated kinematic viscosities and viscosity index at 40° and 100°C of C₃₀-BPAOL lubricant base oils.

Table S4. Reaction specifications.

Table S5. Summary of capital and operating cost for combined production of p -xylene and lubricants.

Table S6. Summary of capital and operating cost.

Fig. S1. Catalysts screening for the synthesis of C₃₀-FL1.

Fig. S2. Effect of catalyst (Aquivion PW98) amount on the yield of C₃₀-FL1 at low and high conversions of reactants.

Fig. S3. Effect of reaction temperature on the production of C₃₀-FL1.

Fig. S4. Arrhenius plot for HAA of 2-pentylfuran with lauraldehyde over Aquivion PW98.

Fig. S5. Time course of the HAA reaction over Aquivion PW98 catalyst.

Fig. S6. Recyclability of Aquivion PW98.

Fig. S7. Time course of the HAA reaction for C₃₀-FL1 synthesis over the P-SiO₂ catalyst.

Fig. S8. Recyclability of P-SiO₂ for the synthesis of C₃₀-FL1.

Fig. S9. Thermogravimetric profiles of P-SiO₂ before and after reaction.
 Fig. S10. Hydrogenation of C₃₀-FL1 over pretreated Pd/C.
 Fig. S11. TEM images of Pd/C before and after reaction.
 Fig. S12. Recyclability of Ir-ReO_x/SiO₂ for the HDO of C₃₀-FL1.
 Fig. S13. TEM images of Ir-ReO_x/SiO₂ before reaction and after 5 cycles.
 Fig. S14. Effect of chain length of 2-alkylfurans on the HAA reaction rate at <25% conversion.
 Fig. S15. Effect of chain length of linear aldehydes on the formation rates of the HAA condensation products at <25% conversion.
 Fig. S16. Effect of aldehyde branching on the formation rates of the HAA condensation products at <25% conversion.
 Fig. S17. Gas chromatogram trace of C₃₀-BPAOL1 and ExxonMobil PAO4.
 Fig. S18. Flow diagram for the production of lubricants from furfural.
 Fig. S19. Overview of cost and impact of raw materials on selling price of lubricants.
 Fig. S20. Overview of cost and impact of raw materials on selling price of lubricants.
 Fig. S21. Distribution of various costs by process.

REFERENCES AND NOTES

- L. R. Rudnick, *Synthetics, Mineral Oils, and Bio-Based Lubricants: Chemistry and Technology* (CRC Press, Taylor & Francis Group, ed. 2, 2013).
- J. C. J. Bart, E. Gucciardi, S. Cavallaro, *Biolubricants: Science and Technology* (Woodhead Publishing Limited, 2013).
- S. Ray, P. V. C. Rao, N. V. Choudary, Poly- α -olefin-based synthetic lubricants: A short review on various synthetic routes. *Lubr. Sci.* **24**, 23–44 (2012).
- U.S. Environmental Protection Agency, "Environmentally Acceptable Lubricants, (EPA 800-R-11-002)" (U.S. Environmental Protection Agency, 2011).
- B. J. Bremmer, L. Plonsker, Bio-based Lubricants: A Market Opportunity Study Update (United Soybean Board, 2008); http://soynewuses.org/wp-content/uploads/MOS_Lubricants2013.pdf.
- R. Buckhalt, press release no.0143.13 and BioPreferred Program Product Categories June 2013 (United States Department of Agriculture, 2013); www.biopreferred.gov/BioPreferred/.
- G. Karmakar, P. Ghosh, B. K. Sharma, Chemically modifying vegetable oils to prepare green lubricants. *Lubricants* **5**, 44 (2017).
- M. A. Hossain, M. A. M. Iqbal, N. M. Julkapli, P. S. Kong, J. J. Ching, H. V. Lee, Development of catalyst complexes for upgrading biomass into ester-based biolubricants for automotive applications: A review. *RSC Adv.* **8**, 5559–5577 (2018).
- N. A. Zainal, N. W. M. Zulkifli, M. Gulzar, H. H. Masjuki, A review on the chemistry, production, and technological potential of bio-based lubricants. *Renew. Sustain. Energy Rev.* **82**, 80–102 (2018).
- J. Haßelberg, A. Behr, Saturated branched fatty compounds: Proven industrial processes and new alternatives. *Eur. J. Lipid Sci. Technol.* **118**, 36–46 (2016).
- M. Balakrishnan, E. R. Sacia, S. Sree Kumar, G. Gunbas, A. A. Gokhale, C. D. Scown, F. D. Toste, A. T. Bell, Novel pathways for fuels and lubricants from biomass optimized using life-cycle greenhouse gas assessment. *Proc. Natl. Acad. Sci. U.S.A.* **112**, 7645–7649 (2015).
- M. Balakrishnan, G. E. Arab, O. B. Kunbargi, A. A. Gokhale, A. M. Grippo, F. D. Toste, A. T. Bell, Production of renewable lubricants via self-condensation of methyl ketones. *Green Chem.* **18**, 3577–3581 (2016).
- M. Gu, Q. Xia, X. Liu, Y. Guo, Y. Wang, Synthesis of renewable lubricant alkanes from biomass-derived platform chemicals. *ChemSusChem* **10**, 4102–4108 (2017).
- D. Jadhav, A. M. Grippo, S. Shylesh, A. A. Gokhale, J. Redshaw, A. T. Bell, Production of biomass-based automotive lubricants by reductive etherification. *ChemSusChem* **10**, 2527–2533 (2017).
- H. Ji, B. Wang, X. Zhang, T. Tan, Synthesis of levulinic acid-based polyol ester and its influence on tribological behavior as a potential lubricant. *RSC Adv.* **5**, 100443–100451 (2015).
- H. Ji, X. Zhang, T. Tan, Preparation of a water-based lubricant from lignocellulosic biomass and its tribological properties. *Ind. Eng. Chem. Res.* **56**, 7858–7864 (2017).
- S. Dutta, A. Bohre, W. Zheng, G. R. Jenness, M. Núñez, B. Saha, D. G. Vlachos, Solventless C–C coupling of low carbon furanics to high carbon fuel precursors using an improved graphene oxide carbocatalyst. *ACS Catal.* **7**, 3905–3915 (2017).
- A. Corma, O. Torre, M. Renz, N. Villandier, Production of high-quality diesel from biomass waste products. *Angew. Chem. Int. Ed.* **50**, 2375–2378 (2011).
- A. Corma, O. Torre, M. Renz, Production of high quality diesel from cellulose and hemicellulose by the Sylvan process: catalysts and process variables. *Energy Environ. Sci.* **5**, 6328–6344 (2012).
- A. D. Sutton, F. D. Waldie, R. Wu, M. Schlaf, L. A. 'Pete' Silks III, J. C. Gordon, The hydrodeoxygenation of bioderived furans into alkanes. *Nat. Chem.* **5**, 428–432 (2013).
- G. Li, N. Li, Z. Wang, C. Li, A. Wang, X. Wang, Y. Cong, T. Zhang, Synthesis of high-quality diesel with furfural and 2-methylfuran from hemicellulose. *ChemSusChem* **5**, 1958–1966 (2012).
- J. P. Lange, E. van der Heide, J. van Buijtenen, R. Price, Furfural—A promising platform for lignocellulosic biofuels. *ChemSusChem* **5**, 150–166 (2012).
- D. S. Park, K. E. Joseph, M. Koehle, C. Krumm, L. Ren, J. N. Damen, M. H. Shete, H. S. Lee, X. Zuo, B. Lee, W. Fan, D. G. Vlachos, R. F. Lobo, M. Tsapatsis, P. J. Dauenhauer, Tunable oleo-furan surfactants by acylation of renewable furans. *ACS Cent. Sci.* **2**, 820–824 (2016).
- C. Gunanathan, D. Milstein, Applications of acceptorless dehydrogenation and related transformations in chemical synthesis. *Science* **341**, 1229712 (2013).
- T. Yokoyama, N. Yamagata, Hydrogenation of carboxylic acids to the corresponding aldehydes. *Appl. Catal. A. Gen.* **221**, 227–239 (2001).
- H. J. Cho, L. Ren, V. Vattipalli, Y.-H. Yeh, N. Gould, B. Xu, R. J. Gorte, R. Lobo, P. J. Dauenhauer, M. Tsapatsis, W. Fan, Renewable *p*-xylene from 2,5-dimethylfuran and ethylene using phosphorus-containing zeolite catalysts. *ChemCatChem* **9**, 398–402 (2017).
- O. A. Abdelrahman, D. S. Park, K. P. Vinter, C. S. Spanjers, L. Ren, H. J. Cho, K. Zhang, W. Fan, M. Tsapatsis, P. J. Dauenhauer, Renewable isoprene by sequential hydrogenation of itaconic acid and dehydra-decyclization of 3-methyl-tetrahydrofuran. *ACS Catal.* **7**, 1428–1431 (2017).
- O. A. Abdelrahman, D. S. Park, K. P. Vinter, C. S. Spanjers, L. Ren, H. J. Cho, D. G. Vlachos, W. Fan, M. Tsapatsis, P. J. Dauenhauer, Renewable isoprene by sequential hydrogenation of itaconic acid and dehydra-decyclization of 3-methyl-tetrahydrofuran. *ACS Sustainable Chem. Eng.* **5**, 3732–3736 (2017).
- Y. Nakagawa, M. Tamura, K. Tomishige, Catalytic reduction of biomass-derived furanic compounds with hydrogen. *ACS Catal.* **3**, 2655–2668 (2013).
- S. Liu, S. Dutta, W. Zheng, N. S. Gould, Z. Cheng, B. Xu, B. Saha, D. G. Vlachos, Catalytic hydrodeoxygenation of high carbon furfurylmethanes to renewable jet-fuel ranged alkanes over a rhenium-modified iridium catalyst. *ChemSusChem* **10**, 3225–3234 (2017).
- S. T. Cui, P. T. Cummings, H. D. Cochran, J. D. Moore, S. A. Gupta, Nonequilibrium molecular dynamics simulation of the rheology of linear and branched alkanes. *Int. J. Thermophys.* **19**, 449–459 (1998).
- J. D. Moore, S. T. Cui, H. D. Cochran, P. T. Cummings, Rheology of lubricant basestocks: A molecular dynamics study of C₃₀ isomers. *J. Chem. Phys.* **113**, 8833 (2000).
- C. McCabe, S. T. Cui, P. T. Cummings, Characterizing the viscosity-temperature dependence of lubricants by molecular simulation. *Fluid Phase Equilib.* **183–184**, 363–370 (2001).
- C. J. Mundy, M. L. Klein, J. I. Siepmann, Determination of the pressure-viscosity coefficient of decane by molecular simulation. *J. Phys. Chem.* **100**, 16779–16781 (1996).
- C. J. Mundy, S. Balasubramanian, K. Bagchi, J. I. Siepmann, M. L. Klein, Equilibrium and non-equilibrium simulation studies of fluid alkanes in bulk and at interfaces. *Faraday Discuss.* **104**, 17–36 (1996).
- A. Karam, K. D. O. Vigier, S. Marinkovic, B. Estrine, C. Oldani, F. Jérôme, High catalytic performance of aquivion PFSA, a reusable solid perfluorosulfonic acid polymer, in the biphasic glycosylation of glucose with fatty alcohols. *ACS Catal.* **7**, 2990–2997 (2017).
- A. Heidekum, M. A. Harmer, W. F. Hoelderich, Addition of carboxylic acids to cyclic olefins catalyzed by strong acid ion-exchange resins. *J. Catal.* **181**, 217–222 (1999).
- M. A. Pérez, R. Bringué, M. Iborra, J. Tejero, F. Cunill, Ion exchange resins as catalysts for the liquid-phase dehydration of 1-butanol to di-n-butyl ether. *Appl. Catal. A. Gen.* **482**, 38–48 (2014).
- R. Weingarten, G. A. Tompsett Jr., W. C. Conner, G. W. Huber, Design of solid acid catalysts for aqueous-phase dehydration of carbohydrates: The role of Lewis and Brønsted acid sites. *J. Catal.* **279**, 174–182 (2011).
- A. J. Jones, S. I. Zones, E. Iglesia, Implications of transition state confinement within small voids for acid catalysis. *J. Phys. Chem. C* **118**, 17787–17800 (2014).
- M. J. Abraham, T. Murtola, R. Schulz, S. Paál, J. C. Smith, B. Hess, E. Lindahl, GROMACS: High performance molecular simulations through multi-level parallelism from laptops to supercomputers. *SoftwareX* **1–2**, 19–25 (2015).
- D. Van Der Spoel, E. Lindahl, B. Hess, G. Groenhof, A. E. Mark, H. J. C. Berendsen, GROMACS: Fast, flexible, and free. *J. Comput. Chem.* **26**, 1701–1718 (2005).
- M. G. Martin, J. I. Siepmann, Transferable potentials for phase equilibria. 1. United-atom description of n-alkanes. *J. Phys. Chem. B* **102**, 2569–2577 (1998).
- M. G. Martin, J. I. Siepmann, Novel configurational-bias Monte Carlo method for branched molecules. Transferable potentials for phase equilibria. 2. United-atom description of branched alkanes. *J. Phys. Chem. B* **103**, 4508–4517 (1999).
- W. W. Wood, F. R. Parker, Monte Carlo equation of state of molecules interacting with the Lennard-Jones potential. I. A supercritical isotherm at about twice the critical temperature. *J. Chem. Phys.* **27**, 720–733 (1957).
- J. I. Siepmann, M. G. Martin, B. Chen, C. D. Wick, J. M. Stubbs, J. J. Potoff, B. L. Eggimann, M. J. McGrath, X. S. Zhao, K. E. Anderson, J. L. Rafferty, N. Rai, K. A. Maerzke, S. J. Keasler, P. Bai, E. O. Fetisov, M. S. Shah, Q. P. Chen, B. Xue, R. F. DeJaco, *Monte Carlo for Complex Chemical Systems-Minnesota, Version 17.1* (University of Minnesota, 2017).
- Q. P. Chen, B. Xue, J. I. Siepmann, Using the k-d tree data structure to accelerate Monte Carlo simulations. *J. Chem. Theory Comput.* **13**, 1556–1565 (2017).

48. S. Nosé, A unified formulation of the constant temperature molecular dynamics methods. *J. Chem. Phys.* **81**, 511–519 (1984).
49. W. G. Hoover, Canonical dynamics: Equilibrium phase-space distributions. *Phys. Rev. A* **31**, 1695–1697 (1985).
50. Y. Zhang, A. Otani, E. J. Maginn, Reliable viscosity calculation from equilibrium molecular dynamics simulations: A time decomposition method. *J. Chem. Theory Comput.* **11**, 3537–3546 (2015).
51. M. P. Allen, *Computer Simulation of Liquids* (Oxford Univ. Press, 1987).
52. W. Humphrey, A. Dalke, K. Schulten, VMD: Visual molecular dynamics. *J. Mol. Graphics* **14**, 33–38 (1996).
53. J. Stone, *An Efficient Library for Parallel Ray Tracing and Animation* (University of Missouri-Rolla, 1998).
54. Z. Lin, V. Nikolakis, M. Ierapetritou, Alternative approaches for p-xylene production from starch: Techno-economic analysis. *Ind. Eng. Chem. Res.* **53**, 10688–10699 (2014).
55. H. M. Jin, E. D. Larson, F. E. Celik, Performance and cost analysis of future, commercially mature gasification-based electric power generation from switchgrass. *Biofuels Bioprod. Biorefin.* **3**, 142–173 (2009).
56. D. Humbird, R. Davis, L. Tao, C. Kinchin, D. Hsu, A. Aden, P. Schoen, J. Lukas, B. Olthof, M. Worley, D. Sexton, D. Dudgeon, *Process Design and Economics for Biochemical Conversion of Lignocellulosic Biomass to Ethanol: Dilute-acid Pretreatment and Enzymatic Hydrolysis of Corn Stover* (National Renewable Energy Laboratory, 2011).
57. F. K. Kazi, A. K. Patel, J. C. Serrano-Ruiz, J. A. Dumesic, R. P. Anex, Techno-economic analysis of dimethylfuran (DMF) and hydroxymethylfurfural (HMF) production from pure fructose in catalytic processes. *Chem. Eng. J.* **169**, 329–338 (2011).
58. BASF, Pricing of precious metals for catalysts (2018); <https://apps.catalysts.basf.com/apps/eibprices/mp/YearlyCharts.aspx>.
59. S. Sadula, A. Athaley, W. Zheng, M. Ierapetritou, B. Saha, Process intensification for cellulose biorefineries. *ChemSusChem* **10**, 2566–2572 (2017).
60. S. Dutta, S. De, B. Saha, M. I. Alam, Advances in conversion of hemicellulosic biomass to furfural and upgrading to biofuels. *Catal. Sci. Technol.* **2**, 2025–2036 (2012).
61. J. Luo, M. Monai, C. Wang, J. D. Lee, D. F. Duchoň, V. Matolin, C. B. Murray, P. Fornasiero, R. J. Gorte, Unraveling the surface state and composition of highly selective nanocrystalline Ni-Cu alloy catalysts for hydrodeoxygenation of HMF. *Catal. Sci. Technol.* **7**, 1735–1743 (2017).
62. R. Ozer, Vapor phase decarbonylation process, WIPO Patent Application WO/2011/026059 (2011).

Acknowledgments: We acknowledge the Advanced Materials Characterization Laboratory at the University of Delaware for providing the TGA facility and W. Zheng for the help with the HR-TEM. **Funding:** This work was supported as part of the Catalysis Center for Energy Innovation, an Energy Frontier Research Center funded by the U.S. Department of Energy, Office of Science, Office of Basic Energy Sciences under award number DE-SC0001004. **Author contributions:** S.L., B.S., and D.G.V. conceived the project and designed the experiments. S.L. executed all the experiments. A.N. reproduced some experiments. T.R.J., Q.P.C., and J.I.S. designed and performed the molecular simulations. A.A. and M.I. performed the techno-economic analysis. S.L., T.R.J., A.A., B.S., and D.G.V. wrote the article. All the authors proofread the manuscript. **Competing interests:** S.L., B.S., and D.G.V. have submitted a Patent Cooperation Treaty patent application as inventors. All the other authors declare that they have no competing interests. **Data and materials availability:** All data needed to evaluate the conclusions in the paper are present in the paper and/or the Supplementary Materials. Additional data related to this paper may be requested from the authors.

Submitted 26 September 2018

Accepted 17 December 2018

Published 1 February 2019

10.1126/sciadv.aav5487

Citation: S. Liu, T. R. Josephson, A. Athaley, Q. P. Chen, A. Norton, M. Ierapetritou, J. I. Siepmann, B. Saha, D. G. Vlachos, Renewable lubricants with tailored molecular architecture. *Sci. Adv.* **5**, eaav5487 (2019).

Renewable lubricants with tailored molecular architecture

Sibao Liu, Tyler R. Josephson, Abhay Athaley, Qile P. Chen, Angela Norton, Marianthi Ierapetritou, J. Ilja Siepmann, Basudeb Saha and Dionisios G. Vlachos

Sci Adv 5 (2), eaav5487.
DOI: 10.1126/sciadv.aav5487

ARTICLE TOOLS	http://advances.sciencemag.org/content/5/2/eaav5487
SUPPLEMENTARY MATERIALS	http://advances.sciencemag.org/content/suppl/2019/01/28/5.2.eaav5487.DC1
REFERENCES	This article cites 51 articles, 2 of which you can access for free http://advances.sciencemag.org/content/5/2/eaav5487#BIBL
PERMISSIONS	http://www.sciencemag.org/help/reprints-and-permissions

Use of this article is subject to the [Terms of Service](#)

Science Advances (ISSN 2375-2548) is published by the American Association for the Advancement of Science, 1200 New York Avenue NW, Washington, DC 20005. The title *Science Advances* is a registered trademark of AAAS.

Copyright © 2019 The Authors, some rights reserved; exclusive licensee American Association for the Advancement of Science. No claim to original U.S. Government Works. Distributed under a Creative Commons Attribution NonCommercial License 4.0 (CC BY-NC).